Journal of Mechanical Science and Technology (KSME Int. J.), Vol. 20, No. 12, pp. 2159~2167, 2006 2159

Consideration of the Frictional Force on the Crack Surface and Its Implications for Durability of Tires

K. -S. Park, T. -W. Kim, H. -Y. Jeong*
Department of Mechanical Engineering, Sogang University,
1 Shinsoo-Dong, Mapo-Gu, Seoul 121-742, Korea
S. -N. Kim
Hankook Tire R & D Center,
23-1 Jang-Dong, Yuseong-Gu, Daejun 305-343, Korea

In order to find out a physical quantity which controls the fatigue life of a structure and to predict the fatigue life of tires, a finite element simulation methodology to use the cracking energy density (CED) and the virtual crack closure technique (VCCT) was proposed and applied to three different tires of a similar size. CED was calculated to predict the location of a crack initiation, and VCCT was used to obtain the strain energy release rate (SERR) at the tip of an initiated crack. Finite element simulations showed that SERR oscillated in the circumferential direction with its minimum occurring just before the contact zone and its maximum occurring just after the center of the contact zone, and SERR was affected significantly by the frictional force acting on the crack surface. In addition, a durability test was conducted to measure the fatigue life of the three tires. The comparison of SERR values with the test data revealed that the fatigue life increased as the amplitude of SERR decreased or as the R-ratio of SERR increased.

Key Words : Tire Durability, Cracking Energy Density, Virtual Crack Closure Technique, Strain Energy Release Rate

1. Introduction

The durability of tires has become one of the most important automotive safety issues since the tire failures of Ford Explorer causing injuries and fatalities (NHTSA, 2001). Thus, when a tire is developed, its durability is to be carefully evaluated by conducting several different types of tests. However, durability test data depend on test methods, and sometimes they scatter widely even under the same test conditions. Thus, research on simulation methodologies to evaluate the durability of a tire or to find out a physical quantity causing a fatigue failure has been conducted (Grosh, 1987; Ebbott, 1996; Wei, 1999; Yan, 2002; Feng, 2004). A crack usually initiates around the belt edge in a tire, and it would grow and cause a catastrophic failure ultimately as a tire is used for a long time (NHTSA, 2001). In order to develop a simulation methodology for tire durability evaluation, it is necessary not only to develop a technique to computationally represent a crack initiation or growth but also to find out a controlling physical quantity (or controlling physical quantities) in the fatigue failure process. Physical quantities such as the strain energy density (SED), the effective stress, the first invariant of the Cauchy-Green deformation tensor, the maximum principal nominal strain were evaluated, and SED seemed to be a controlling physical quantity (Roberts,

* Corresponding Author,
E-mail : jeonghy@sogang.ac.kr
TEL : +82-2-705-8640; **FAX** : +82-2-712-0977
Department of Mechanical Engineering, Sogang University, 1 Shinsoo-Dong, Mapo-Gu, Seoul 121-742, Korea.
(Manuscript **Received** June 1, 2006; **Revised** October 27, 2006)

1977; Ro, 1989; DeEskinaze, 1990; Choi, 2005).

However, some test data showed that uniaxial tension specimens and biaxial tension specimens with the same SED resulted in different fatigue life (Roberts, 1977; Roach, 1982), implying that SED is not a controlling physical quantity in a fatigue failure. Thus, it was proposed to consider only the strain energy stored with respect to a feasible crack plane because only the strain energy stored with respect to a crack plane rather than the whole strain energy would be released if a crack initiated on the plane (Mars, 2001). In other words, in a structure subjected to loading there exists a plane at a location where CED has its maximum, and it is most likely for a crack to initiate at the location along the plane. Once a crack initiates, it usually grows under continuous loading. Fatigue life usually depends on the growth rate of a crack, which is usually represented by the Paris law to use the amplitude of a physical quantity such as SERR. VCCT has been used to obtain the value of SERR for an existing crack (Rybicki, 1977; Shivakumar, 1988; Liebowitz, 1989), and it is also used in this paper.

In order to apply the simulation methodology for the fatigue failure analysis of tires, finite element (FE) models of three different tires of a similar size were created. Then, the location and plane for which CED had its maximum was determined, and a crack was created at the location on the plane. Finally, VCCT was applied to calculate SERR at the tip of the crack, and SERR was obtained with the tire being rotated by some degrees in order to find out the SERR as function of the rotation angle. In addition, a durability test was conducted for the three tires. The comparison of SERR as function of the rotation angle and the durability test data revealed that the fatigue life of the three tires increased as the amplitude of SERR decreased or the R-ratio of SERR increased.

2. Physical Quantities for the Crack Initiation and Growth

2.1 Cracking energy density

SED has been regarded as a controlling physical quantity in the fatigue failure and used in many fatigue failure analyses (Beatty, 1964; Ro, 1989; DeEskinaze, 1990). For a rubber bushing, SED turned out to be a better predictor for fatigue life than the effective stress, the first invariant of the Cauchy-Green deformation tensor or the maximum principal nominal strain (Choi, 2005). However, some experimental results showed that natural rubber specimens under equibiaxial tension resulted in about four times longer fatigue life than those under uniaxial tension even though they had the same SED (Roberts, 1977; Roach, 1982). This means that the amount of energy released due to crack initiation or growth depends on loading conditions, and SED may not be a controlling physical quantity in a fatigue failure of a structure especially under combined loading conditions. Thus, it is necessary to calculate the strain energy released due to crack initiation or growth rather than the strain energy stored in a structure (Mars, 2001). In other words, the plane and location of a crack should be taken into account in the calculation of the released strain energy.

CED is only a part of SED to be released as a crack initiates or grows, and it depends on the crack plane as well as the crack location. Note that CED can be defined not only for an actual crack plane but also for a (virtual) plane where a crack is likely to occur. In Fig. 1, a stress vector, a strain increment vector and a normal vector of a crack plane are shown. The stress vector (or the strain increment vector) can be readily obtained from a linear transformation of the normal vector by the stress tensor (or the strain increment tensor). Then, the CED increment can be calculated from

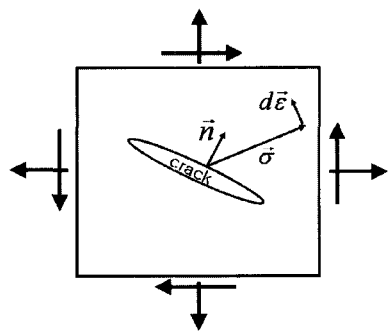

Fig. 1 Stress vector, strain increment vector and the normal vector of a crack

the dot product between the stress vector and the strain increment vector as shown in Eq. (1), and CED can be obtained by integrating the CED increment during a loading history as shown in Eq. (2) (Mars, 2001).

$$dW=\vec{n}^T\underline{\sigma}\,d\underline{\varepsilon}\,\vec{n}=\vec{\sigma}d\vec{\varepsilon} \tag{1}$$

$$W=\int_0^{\varepsilon}\vec{\sigma}d\vec{\varepsilon} \tag{2}$$

Here, $\underline{\sigma}$ is the stress tensor, $d\underline{\varepsilon}$ is the strain increment tensor, $\vec{\sigma}$ is the stress vector, $d\vec{\varepsilon}$ is the strain increment vector, and $\vec{n}$ is the normal vector. It is noteworthy that it is likely for a crack to initiate or grow along the plane at a location where CED has its maximum (Mars, 2001).

SED and CED were calculated for a uniaxial tension specimen and for an equibiaxial tension specimen used for the fatigue tests (Roberts, 1977; Roach, 1982), and they are shown in Fig. 2. Note that CED for an equibiaxial tension specimen is a half of that for a uniaxial tension specimen even though SED is the same. Thus, CED seems to be in a better correlation than SED with the fatigue test data which showed that the fatigue life of equibiaxial tension specimens was about four times longer than that of uniaxial tension specimens.

2.2 Strain energy release rate and virtual crack close technique

When a crack grows in a structure, the strain energy stored in the structure decreases. The strain energy decreased during crack growth per unit area of new crack surface is the strain energy release rate (SERR), which is an indicator how strongly a crack tends to grow. It was proposed that the strain energy released during crack growth was the same as the energy required to close the crack growth (Irwin, 1957), and this technique, called the virtual crack closure technique (VCCT), has been used in many derivations for SERR (Rybicki, 1977; Shivakumar, 1988; Liebowitz, 1989).

In Fig. 3, a schematic diagram for crack growth and virtual crack closure is shown. Suppose that a crack grows by Δa, the node at the crack tip splits into two nodes f and g, the force at the crack tip before the crack growth is $\vec{F}$, and the relative displacement between the two nodes is $\Delta\vec{u}$. Using VCCT, SERR denoted by G can be approximately calculated by Eq. (3) using the components of $\vec{F}$ and $\Delta\vec{u}$, which is easily applicable in FE simulations (Rybicki, 1977).

$$G=\frac{1}{2\Delta a}[F_x\Delta u_x+F_y\Delta u_y+F_z\Delta u_z] \tag{3}$$

Note that the force $\vec{F}$ in Eq. (3) is assumed to linearly decrease to $\vec{0}$ during the crack growth, and Δa should be small enough.

In order to evaluate the validity of VCCT, an FE model was created using plane strain elements for a single edge cracked specimen shown in Fig. 4. SERR was obtained for the specimen under the Mode I plane strain conditions by using VCCT, and then it was compared with that obtained from the J-integral or the theoretical solutions. It is well known that the J-integral is valid for a linear or nonlinear elastic material under the plane

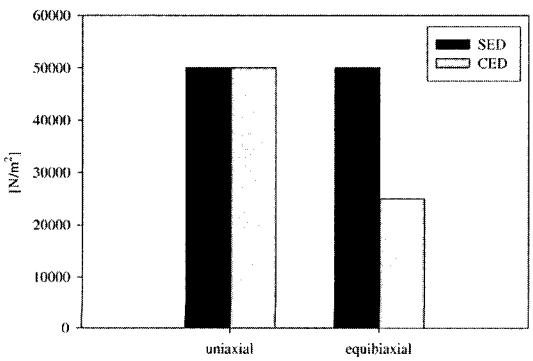

Fig. 2 SED and CED of a specimen under uniaxial tension or equibiaxial tension

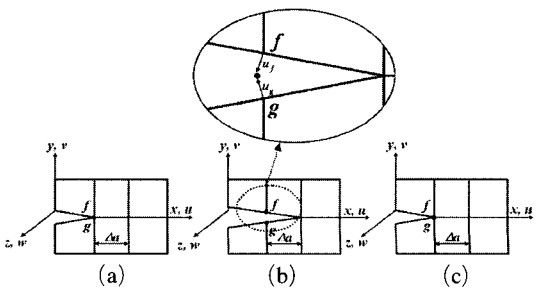

Fig. 3 Schematic diagram of the virtual crack closure technique

strain conditions (Rice, 1968). In addition, the theoretical solution for the stress intensity factor for the tensile specimen is given as Eq. (4), and SERR can be obtained from Eq. (5) with the assumption of the specimen being in the plane strain state.

$$K_I=\frac{P}{B\sqrt{W}}\frac{2\tan\frac{\pi a}{2W}}{\cos\frac{\pi a}{2W}}\left[0.752+2.02\left(\frac{a}{W}\right)+0.37\left(1-\sin\frac{\pi a}{2W}\right)^3\right] \quad (4)$$

$$G=\frac{K_I}{E/(1-v^2)} \quad (5)$$

Here, P/B is the load per unit thickness, W is the width, a is the crack length, and v is the Poisson's ratio. Note that a fine mesh with 2nd-order quadrilateral elements satisfying the $r^{-1/2}$ singularity around the crack tip was used for the J-integral, but a comparatively coarse mesh with 1st-order quadrilateral elements was used for VCCT. In Table 1, SERR's obtained from the theoretical solutions, the J-integral and VCCT are shown. Since the three solutions are close to one another, it can be said that VCCT results in a reasonable amount of SERR at least for a crack under Mode I, and it is easier to use than the J-integral because the number of elements used was smaller and only 1st-order quadrilateral elements were used. It is also noteworthy that unlike J-integral VCCT is applicable not only to a crack in plane strain or plane stress conditions but also to a crack under 3-dimensional loading conditions.

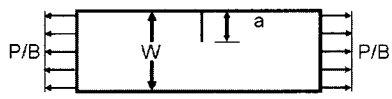

Fig. 4 A single edge cracked specimen

Table 1 SERR for a plane strain specimen under Mode I obtained from theoretical solutions, J-integral and VCCT

	Theoretical	J-integral	VCCT
G [N/m]	233.60	230.73	234.32

2.3 Strain energy release rate for a crack with a frictional force

When a crack is subjected to compression, a frictional force should be taken into account in the calculation of SERR because it causes some energy loss. In order to analyze the effect of friction on the stress field and SERR for the crack, a plane strain specimen with a crack shown in Fig. 5 was simulated both with no friction and with the coefficient of friction of 0.5. Only a half model with the symmetric plane at the left was created with displacement boundary conditions of -2 mm on the top surface and of 1 mm on the right upper side surface. Due to Poisson's effect, the lower right side surface deformed to the right more than 1 mm, and the displacement boundary condition on the right upper side surface actually prevented the upper half from deforming freely.

The contour plots of the effective stress around the crack tip were obtained from the simulations, and they are shown for the case of no friction and for the case of friction in Fig. 6(a) and (b), respectively. The effective stress around the crack was clearly lower for the case of friction than for the case of no friction. SERR's were also calculated by using the J-integral and VCCT for the

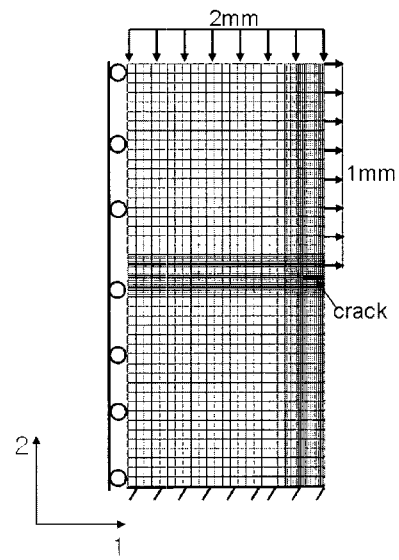

Fig. 5 A crack in a plane strain specimen under compression

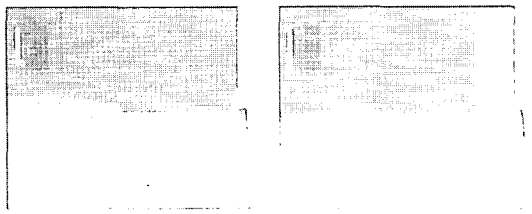

(a) (b)

Fig. 6 Contour plot of the effective stress (a) no friction (b) friction

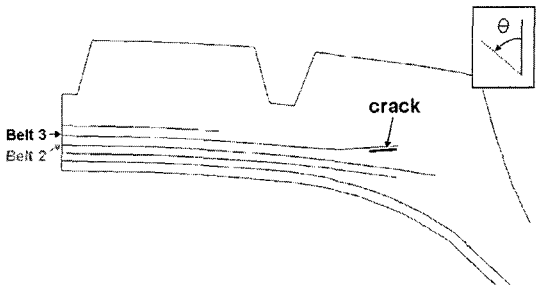

Fig. 7 Location of the maximum CED in Tire A

Table 2 SERR for a plane strain specimen under compression obtained from J-integral and VCCT

	no friction	friction
J-integral [N/m]	128.04	41.96
VCCT [N/m]	128.28	41.52

FE model, and they are shown in Table 2. Note that SERR for the case of friction was about a third of that for the case of no friction. Therefore, it can be said from the contour plots and SERR that friction prevents a crack from growing. Note also that SERR's obtained from VCCT were very close to those from the J-integral both for the case of no friction and for the case of friction.

3. Application to Tires

3.1 Location and plane for crack initiation

A crack usually occurs around the belt edge in a tire. As a tire rotates, the crack is subjected to cyclic loading of compression, tension and shear, and it grows circumferentially and laterally, causing a catastrophic failure ultimately. In this study the durability of three different tires of a similar size, named Tire A, B, and C, was evaluated using CED and VCCT (Kim, 2005). In order to determine a feasible location of crack initiation, CED needed to be calculated all over the tires. Note that CED depends on the location and the angle, and the plane for which the maximum CED occurs can be regarded as the plane for crack initiation or growth. The plane where the maximum CED occurred in Tire A, as an example, is shown in Fig. 7, and the maximum CED value and the angle of the plane are shown for all the three tires in Table 3. In all the three tires the maximum CED occurred just inside the edge of belt #3 and its plane was almost parallel to the belt. It is noteworthy that the location and the plane for the maximum CED are compatible with observations for crack initiation sites (NHTSA, 2001).

Table 3 Location and angle of the maximum CED

	Tire A	Tire B	Tire C
Crack angle [deg]	94	95	94
CED [N/m^2]	159535	293000	229000

3.2 Strain energy release rate calculation using virtual crack closure technique

It has been believed for a long time that crack growth is related to SERR. In order to calculate SERR for a crack by using VCCT, it is not necessary to have fine mesh all over the tire. Rather, it is more efficient to conduct a global-local analysis (Ebbott, 1996). A coarse mesh was used first for the entire tire, and then a fine mesh was used only for the elements around the crack, the displacement field obtained from the first simulation being imposed on the boundary of the fine mesh. The coarse mesh and the fine mesh used for Tire A, as an example, are shown in Fig. 8. In the fine mesh an initiated crack was made on the plane at the location determined in Sec. 3.1, and the initial crack size was assumed to be 12.5 mm wide (laterally) and 35 mm long (circumferentially).

Of course, in order to consider the frictional force occurring on the crack surface under compression in a tire, it was necessary to conduct a test to determine the coefficient of friction at high

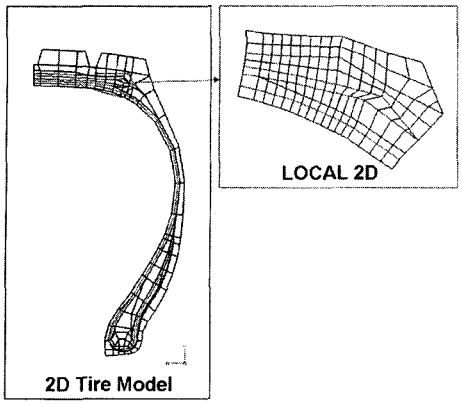

Fig. 8 Coarse mesh and fine mesh used in the global-local analysis

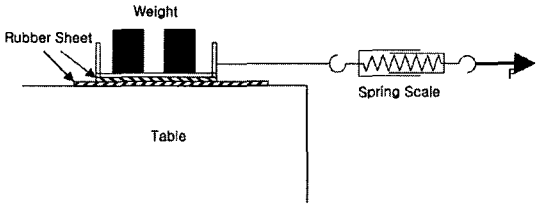

Fig. 9 A friction test set-up

temperature as well as room temperature since the temperature around the edge increases during a durability test. As shown in Fig. 9, a couple of rubber sheets were compressed by a dead weight while they were heated by a heat blower. When the temperature around the rubber sheets reached 35℃, 50℃ or 70℃, the upper rubber sheet was pulled by a spring scale and the force at the moment when the upper rubber sheet started to move was measured. The coefficient of friction was determined as the ratio of the pulling force to the weight on the top, and it is shown for four different temperatures in Fig. 10. The coefficient of friction was proven to depend heavily on the temperature, but it was chosen to be 1 for this study since the average value of it was about 1.

SERR was efficiently calculated by using VCCT and Eq. (3). Note here that SERR is the strain energy loss per unit area of new crack surface as the new crack surface area approaches zero and it may depend on the mesh size. Thus, in this study the mesh sensitivity of SERR was also evaluated. The initial mesh was reduced to a half in the second mesh. the second mesh was reduced to a half

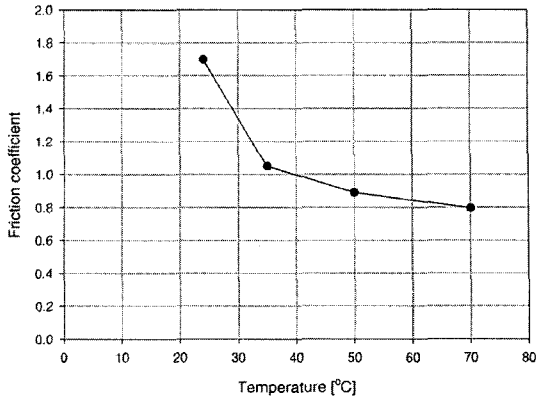

Fig. 10 Coefficient of friction as function of temperature

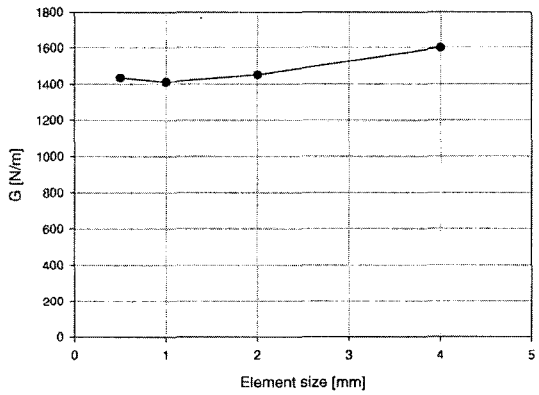

Fig. 11 SERR for four different mesh sizes

in the third mesh, and finally the third mesh was reduced to a half in the fourth mesh. Then, SERR was calculated for all the four meshes, and their SERR's are shown in Fig. 11. Since SERR did not change significantly from the second mesh, it was determined to use the mesh size of about 2 mm used in the second mesh for the SERR calculation.

3.3 Amplitude and R-ratio of SERR, and fatigue test data

As a tire rotates, a crack also rotates and consequently SERR around a crack varies. It is easy to believe but not true that SERR around a crack has its maximum when the crack is at the bottom (i.e., in the contact zone) and it has its minimum when the crack is at the top. In order to figure out the variation of SERR due to the tire rotation, a

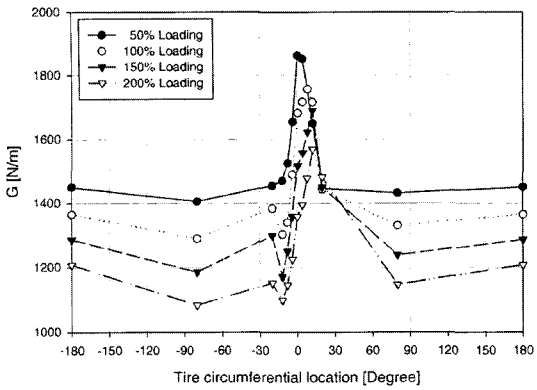

Fig. 12 SERR as function of the circumferential angle for four different loadings

tire with a crack was rotated from the center of the contact zone, and SERR was calculated. SERR was calculated for all the three tires under four different loadings of 50%, 100%, 150% or 200% of the nominal load. As an example, SERR is shown as function of the rotation (or circumferential) angle for Tire A under four different loadings in Fig. 12, where the angle is measured from the center of the contact zone. It is clear in Fig. 12 that SERR has its minimum just before the contact zone and its maximum just after the center of the contact zone. From the minimum and maximum of SERR, the amplitude and R-ratio defined as the ratio of the minimum to the maximum could be calculated, and they are shown in Fig. 13(a) and (b), respectively, for all the three tires. Except the loading of 50%, the amplitude of SERR was ranked in the following order for Tire A, Tire B and Tire C. However, R-ratio was ranked in the following order for Tire C, Tire B and Tire A. It is well known that a natural rubber shows a longer fatigue life when the R-ratio is higher for the same maximum load or displacement (Lidley, 1974; Gent, 2001; Legorju-jago, 2002). It stems from the crystallization occurring at the crack tip, which behaves as a barrier, preventing a crack from growing through (Treloar, 1958; Lidley, 1974).

A durability test of which the load was 140% of the nominal loading was conducted for all the three tires, and the test data are shown in Table 4. By comparing the amplitude and the R-ratio of

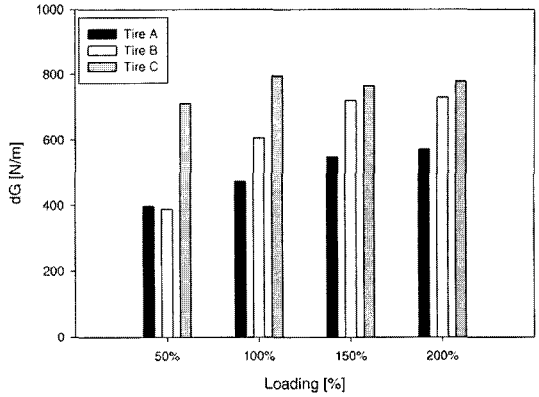

(a)

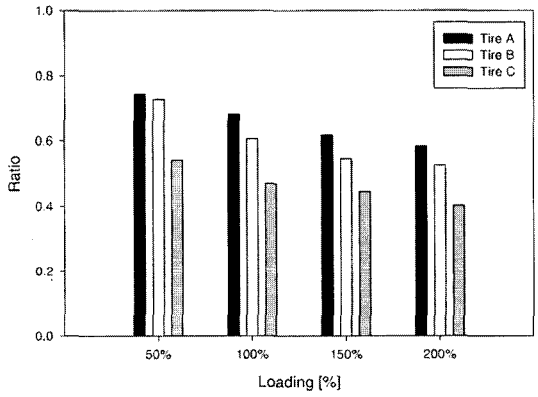

(b)

Fig. 13 (a) Amplitude of SERR for four different loadings (b) R-ratio of SERR for four different loadings

Table 4 Durability test data

	Tire A	Tire B	Tire C
Time [hr]	342	107	42

SERR with the test data, it can be noticed that the smaller the amplitude of SERR is or the higher the R-ratio of SERR is, the longer the fatigue life is. Since the amplitude or the R-ratio of SERR is at least qualitatively in a good correlation with the fatigue test data, either one of them can be regarded as a controlling physical quantity in a fatigue failure process.

4. Conclusions

A simulation methodology using CED and VCCT was proposed for a fatigue failure analysis

in this paper, and the accuracy of this methodology was evaluated by applying the methodology to three different tires and comparing qualitatively the simulation results with the durability test data. It was found that CED had its maximum just inside the edge of the third belt of all the three tires. Thus, a crack was created at the location in the FE models of the three tires, and SERR was calculated by using VCCT. It is noteworthy that SERR had its minimum just before the contact zone and its maximum just after the center of the contact zone. By comparing the amplitude and R-ratio of SERR with the durability test data of the tires, it was found out that the fatigue life of the three tires increased as the amplitude of SERR decreased or as the R-ratio of SERR increased. Therefore, it can be said that the methodology developed in this paper was successfully applicable to tires, and the amplitude or the R-ratio of SERR was at least qualitatively in a good correlation with the durability test data.

References

Beatty, J. R., 1964, "Fatigue of Rubber," *Rubber Chemistry and Technology*, Vol. 37, pp. 1341~1364.

Choi, J. -H, Kang, H. -J., Jeong, H. -Y., Lee, T. -S. and Yoon, S. -J., 2005, "Heat-Aging Effects on the Material Property and the Fatigue Life of Vulcanized Natural Rubber, and Fatigue Life Prediction Equations," *Journal of Mechanical Science and Technology*, Vol. 19, No. 6, pp. 1229~1239.

DeEskinazi, J. and Ishihara, K., 1990, "Towards Predicting Relative Belt Edge Endurance with Finite Element Method," *Tire Science and Technology, TSTCA*, Vol. 18, No. 4, pp. 216~235.

Ebbott, T. G., 1996, "An Application of Finite Element-Based Fracture Mechanics Analysis to Cord-Rubber Structure," *Tire Science Technology, TSTCA*, Vol. 24, No. 3, pp. 220~235.

Feng, X. and Yan, X., 2004, "Analysis of Extension Propagation Process of Interface Crack between Belts of a Radial Tire Using a Finite Element Method," *Applied Mathematical Modelling*, Vol. 28, pp. 145~162.

Gent., N., 2001, *Engineering with Rubber*, 2nd edition, HANSER, Cincinnati, pp.137~176.

Grosh, K., 1987, "Rolling Resistance and Fatigue Life of Tires," *Rubber Chemistry and Technology*, Vol. 61, pp. 43~63.

Irwin, G. R., 1957, "Analysis of Stresses and Strains Near the End of a Crack Traversing a Plate," *Journal of Applied Mechanics*, Vol. 24, pp. 361~364.

Kim, T. -W., Jeong, H. -Y., Choe, J. -H. and Kim, Y. -H., 2005, "Prediction of the Fatigue Life of Tires Using CED and VCCT," *Key Engineering Materials*, Vol. 297~300, pp. 102~107.

Legorju-jago., K. and Bathias, C., 2002, "Fatigue Initiation and Propagation in Natural and Synthetic Rubbers," *International Journal of Fatigue*, Vol. 24, pp. 85~92.

Liebowitz, H. and Moyer, E.T., 1989, "Finite Element Methods in Fracture Mechanics," *Comput. Struct*, Vol. 31, No. 1, pp. 1~9.

Lindley, P. B., 1974, "Non-Relaxing Crack Growth and Fatigue in a Non-Crystallizing Rubber," *Rubber Chemistry and Technology*, Vol. 47, pp. 1253~1264.

Mars, W. V., 2001, "Multiaxial Fatigue Crack Initiation in Rubber," *Tire Science and Technology, TSTCA*, Vol. No. 3, pp. 171~185.

NHTSA, ODI, 2001, "Engineering Analysis Report and Initial Decision Regarding EA00-023 : Firestone Wilderness AT Tires."

Rice, J., 1968, "A Path Independent Integral and the Approximate Analysis of Strain Concentration by Notches and Cracks", *Journal of Applied Mechanics*, Vol. 35, pp. 379~386.

Ro, H. S., 1989, *Modeling and Interpretation of Fatigue Failure Initiation in Rubber Relater to Pneumatic tires*, Ph.D. Dissertation, Purdue University.

Roach, J. F., 1982, *Crack Growth in Elastomers under Biaxial Stresses*, Ph.D. Dissertation, University of Akron.

Roberts, B. J., 1977, "The Relationship between Uniaxial and Equibiaxial Fatigue in Gum and Carbon Black Filled Vulcanizates," *Proceedings of Rubbercon'77*, Vol. 2.1, pp. 2.1~2.13.

Rybicki, E. F., 1977, "A Finite Element Calculation of Stress Intensity Factors by A Modified

Crack Closure Integral," *Engineering Fracture Mechanics*, Vol. 9, pp. 931~938.

Shivakumar, K. N., 1988, "A Virtual Crack Closure Technique for Calculating Stress Intensity Factors for Crack Three Dimensional Bodies," *International Journal of Fracture*, Vol. 36, pp. R43~R50.

Treloar., L. R. G., 1958, *Physics of Rubber Elasticity*, Oxford University Press, London

Wei, Y. -T.,Tian, Z. -H., and Du, X. W., 1999, " A Finite Element Model for Rolling Loss Prediction and Fracture Analysis of Radial Tires," *Tire Science Technology, TSTCA*, Vol. 27, No. 4, pp. 250~276.

Yan, X. and Wang, Y., 2002, "Study for the Endurance of Radial Truck Tires with Finite Element Modeling," *Mathematics and Computers in Simulation*, Vol. 59, pp. 471~488.